

Durability Based Design of FRP Jackets for Seismic Retrofit

by

R. Walker, Wetherford & Associates;
V.M. Karbhari, University of California San Diego

Abstract

This paper provides results of an investigation aimed at assessing the effect of deterioration over time, at the materials level, on the effectiveness of fiber reinforced polymer (FRP) jacket used for seismic retrofit. Three different systems are investigated and results from an accelerated test program are used to provide predictive equations of long-term performance of the material, which are then used to analyze effectiveness at the level of seismic retrofit. The effect of deterioration is expressed, for ease in comparison, to an increase in the required thickness of the jacket for the required level of service-life. The use of the proposed methodology is shown to not only enable a better assessment of jacket design but to also allow for assessment of dominant mechanisms controlling selection of thickness which can change with time of exposure. It is demonstrated that for the case of seismic retrofit the use of current ACI-440 durability factors could be overly conservative.

Introduction

Concrete columns that need to be retrofit are commonly deficient in flexural ductility, shear strength, bar buckling restraint, and/or lap splice clamping. Jacketing has been effected through the application of steel shells, additional reinforced concrete, and the wrapping of fiber reinforced polymer (FRP) composites around the deficient column. While all three methods provide the required retrofit efficiency FRP composites offer significant advantages as related to speed of application, substantially less disruption of traffic, reduced weight, insignificant change to dimensions and the overall configuration, potentially lower life-cycle maintenance, and directional anisotropy. Since the efficacy of the jacket is dependent on hoop confinement FRP composites offer tremendous tailorability since they can be designed to have fibers oriented primarily in the hoop direction to provide constraint without substantially increasing stiffness over the height of the column.

The effectiveness of FRP jacketing has been extensively validated through large and full-scale laboratory tests (Seible et al, 1997; Xiao and Ma, 1997; Saiidi et al, 2004), field applications (Pantelides et al, 2004) and in-situ field tests and assessment (Pantelides et al, 1999; Pantelides and Gergely, 2002). In addition significant research has been conducted in developing an understanding of the mechanisms of interaction between the FRP jacket and the concrete and the overall retrofit response. To date advances have also been made in the development of design guidelines and specifications including for construction (ACI-440, 2002; Caltrans, 1996; Mirmiran et al., 2004; TR-55, 2000). While the structural effectiveness of FRP jackets has been widely accepted by the community there is still some reservation regarding its use due to concerns related to cost and long-term durability in field environments.

In recent years, durability of FRP jacketing materials has been assessed through laboratory tests (Karbhari et al, 2003; Zhang et al., 2003a; Saenz et al, 2005a; Saenz et al, 2005b) and limited field tests (Zhang et al, 2003b) and a detailed set of evaluation criteria and durability test protocols have been established by the Civil Engineering Research Foundation under the aegis of the Federal Highway Administration (Reynaud et al, 1999). This research has, however, largely been at the level of materials deterioration and has not been linked to the design, or assessment of deterioration, at the structural level. If deterioration rates for a specific FRP composite were known jackets could be designed with an appropriate safety factor, accomplished through use of "sacrificial" thickness, to ensure their reliability over expected periods of field use. This paper reports on the results of an investigation aimed at providing a means for this as well as a basis for the future development of reliability based design tools that incorporate materials deterioration.

Materials Systems and Test Methods

Three different systems, representative of commercially available products that have been used extensively in the field were investigated. System A is representative of the prefabricated class wherein a hollow circular cross-sectional shell is first fabricated under carefully controlled factory conditions, including elevated temperature cure over an extended period of time. This cylinder is then slit down the length to create an opening and after the addition of adhesive to the inner surface is pulled over a column. Subsequent layers are added with the position of the slit being staggered to enable good overlap with the overall configuration being akin to that of an onionskin. Bonding is achieved under ambient conditions with external pressure applied by separate circumferential straps tightened manually and removed after a period of time. Systems B and C are representative of the extensively used wet layup process. The primary

difference between these systems was that system B used Aramid tows in the transverse direction whereas system C was completely constituted of E-Glass fibers. The volume fraction of transverse direction fibers in both cases was extremely small with the fibers essentially serving to hold the warp direction fibers in place. All three systems considered in this investigation were primarily of unidirectional orientation with the reinforcing fibers being of E-glass.

In order to capture materials, manufacturing and structural aspects in a single coupon (Reynaud et al, 1999; Zhang et al, 2003) the ring burst test was used in this investigation. The 510 mm (20" internal diameter) rings allowed the stressing of the material in a fashion closely simulating the actual structural system during dilation of concrete during a seismic event. Following procedures detailed by Reynaud et al. (1999), specimens were fabricated by manufacturers as in the field, in the form of blanks of 178 mm (7") height, to enable the system to be exposed to environmental conditions in the jacket, rather than ring, configuration. All blanks were coated in the same manner as would be applied in the field to provide protection against environmental exposure and all edges were sealed using the same coating. Specimens were immersed in water at 15°C, 23°C, 40°C and 60°C for extended periods of time to enable use of time-temperature superposition principles for prediction of long-term durability. Base-line specimens were also stored under controlled conditions of 23°C and 55% relative humidity (RH).

Once exposures were completed, 4 rings each of 25.4 mm (1") height were cut from the central portion of each blank (Figure 1) with a fifth ring being also cut from the same section for specimens to be tested in short-beam-shear (SBS) using specimens of nominal span-to-depth ratio of 5:1, assessment of glass transition temperature (T_g), moisture content, and microscopic investigations. The use of test specimens from the central region of each test blank, rejecting edge areas, enabled almost complete elimination of edge effects during environmental exposure which could, otherwise, have resulted in non-uniformity; and testing of specimens with moisture contents and attendant damage not likely to be encountered by the overall jacket in the field. In order to provide a standard baseline for design of test specimens for purposes of durability assessment, a predetermined internal pressure rating of 17.2 MPa (2500 psi) with a maximum thickness constraint of 11.5 mm (0.45") following specifications prescribed by the California Department of Transportation (Caltrans, 1996) was set.

Results of Durability Testing And Arrhenius Analysis

Details related to dominant damage mechanisms for each of the systems were reported earlier by Karbhari et

al. (2003) and are hence not repeated herein. Results of the exposures for each of the systems are summarized in Tables 1-3.

Since the reinforcing shells in system A were fabricated under controlled conditions with elevated temperature cure the weak link in terms of degradation due to environmental exposure is the ambient cured adhesive. Failures were seen in all cases within the adhesive layer, with very little damage to the prefabricated layer surfaces. As a result of exposure, system B samples showed mechanisms of delamination between fabric layers with significant hoop splitting and tearing of fabric accompanied by pull-out of the aramid tows at lower temperatures and upto the 12 month period at 60°C, after which failure was due to fiber rupture indicating deterioration of fiber-matrix bond and even of the fiber. In comparison to system B, the transverse tows in system C fabric were also from E-glass which could be expected to result in less swelling and moisture uptake as compared to that resulting from the aramid fibers. Levels of deterioration are seen to be slightly less than that of system B at the two lower temperatures of 15°C and 23°C but are higher with a faster rate of deterioration at the two higher levels of 40°C and 60°C. In all cases failure was through a combination of separation between layers and tensile rupture with some degradation at the longer time periods at the fiber and fiber-matrix interphase level.

Following the procedure in Litherland et (1981), Proctor et al (1982) and as recently used for E-glass vinylester systems by Chin et al. (2001) and Karbhari (2004), the Arrhenius method was used to predict changes in performance over time. In this method the logarithm of time to reach a set of levels of percentage retention versus $1/T$ (where T is the temperature in Kelvin) is used to predict service life at a given temperature (normally assumed to be the ambient level). This follows from the Arrhenius rate equation which shows first-order effects, wherein it is assumed that the rate at which degradation occurs follows the form

$$k = A \exp\left(\frac{-E_a}{RT}\right) \quad \dots(1)$$

where k is a variable representing the rate of degradation, E_a is the activation energy, R is the universal gas constant, and T is the exposure temperature in degrees Kelvin. The validity of the primary assumption, that the material has a set of dominant mechanisms which do not change with time and temperature, but are accelerated by increase in temperature, is borne out through a linear relationship between the diffusion coefficients for the materials immersed at various temperatures and the temperature of immersion. Using data from tests conducted at 15, 40 and 60°C, predictions were made for property retention as a function of time for the 23°C immersion case, and are seen to compare well with the experimental results for this exposure within the overall scatter

bounds. Equations for time dependent change in properties for the three material systems are given in Table 4.

It is noted that immersion in water represents a single exposure condition which may not represent exposure in the field. The results of the durability of system A and B materials through field exposure adjacent to actual wrapped bridge columns in Tacoma, Washington, were reported earlier by Zhang et al. (2002). The exposure for the period of 89 weeks included temperature variation between -2°C and 35.6°C , with precipitation, freeze-thaw cycles, and salt exposure from road salt. A comparison of data from field exposure and the predictions for immersion in water at 23°C (based on equations in Table 4) shows that for system A the rate coefficients due to field exposure for strength and modulus need to be modified by 0.625 and 1.129, respectively, and those for system B by 0.646 and 1.877, respectively. This shows that the specific field environment considered in that study is replicated rather closely by the immersion environment considered herein with the strength deterioration being slightly slower in the field than as indicated by acceleration, and the modulus deterioration actually being faster in the field than indicated by deterioration.

Comparison With ACI-440 Recommendations

The American Concrete Institute guidelines (ACI-440, 2002) suggest that the design ultimate strength, f_{fu} , be determined by modifying the reported strength, f_{fu}^* , by an environmental reduction factor, C_E , such that

$$f_{fu} = C_E f_{fu}^* \quad \dots (2)$$

where

$$f_{fu}^* = (\bar{f}_{fu} - 3\sigma) \quad \dots (3)$$

\bar{f}_{fu} is the mean ultimate strength and σ is the standard deviation of the test population. For cases of exterior exposure and aggressive environments, $C_E = 0.65$, indicating that the threshold to which the FRP composite can degrade prior to being considered as below the reported value is $0.65 f_{fu}^*$. A similar restriction exists for design rupture strain. ACI-440 (2002), however, assumes that modulus is not affected by environmental conditions and hence the design allowable is taken to be the value reported by the manufacturer, i.e. the average determined through testing. A comparison of the ACI recommended values with predictions from the equations determined through accelerated testing are shown in Table 4 for the three systems considered in the current investigation. Since the thickness of FRP composite jackets can be shown to relate directly to the modulus of the composite in the cases of shear strength retrofit and lap-splice clamping (Seible and Karbhari, 1997) and the modulus in the case of the systems considered herein does degrade over time (even over the short-term) the approach listed in equations (2) and (3) is used for modulus as well in

this paper, which is in line with the guidelines from the Concrete Society in the UK (TR-55, 2000).

As can be seen from Table 5, the ACI-440 (2002) values are significantly lower than the nominal values determined from the as-received (i.e. without exposure) tests on the three systems. Use of the predictive equations determined through accelerated testing also shows that in the case of modulus and ultimate strain the ACI-440 values are not reached for extremely long periods of time. Since there is intrinsically a concern related both to the use of accelerated tests and the extrapolation of short-term data to extremely long periods of time the values are simply given as “> 100 years.” It should, however, be emphasized that these predictions are made based on the assumption of continuation of self-similar behavior without changes in damage mechanisms over time. As can be seen, system A shows the least amount of time required to reach the ACI value for strength, whereas system C does not show deterioration to that level within the nominal 100 year period. As noted previously the presence of the aramid fibers causes both increased moisture wicking and degradation along the interface which explains why system B takes a significantly lower time to reach the ACI value than system C. It should be mentioned that these values are determined from the perspective of immersion in water at 23 C. In reality exposure conditions in the field would consist of variation in environment, resulting, in general, in a slightly different rate of deterioration. A comparison based on the use of factors determined from the limited field data reported by Zhang et al. (2002) and reported in the previous section indicates that the ACI values for strength would be reached in the field in 23.68 years and 31.74 years for systems A and B, respectively.

Background to Jacket Design

Reinforced concrete columns with insufficient transverse reinforcement and/or seismic detailing show three primary failure modes. Six design regions can be defined based on these modes. They are L_s , the lap splice length, L_{c1} , the primary confinement region for plastic hinge, L_{c2} , the secondary confinement region adjacent to the plastic hinge, L_v , the shear strengthening region where L_v^l is the shear retrofit inside the plastic hinge zone and L_v^o is the shear retrofit outside the plastic hinge zone (Seible and Karbhari, 1997). To date a significant number of approaches have been proposed for the design of FRP jackets for column retrofit and reviews have been recently reported by Teng et al. (2002) and will hence not be repeated herein. For the purposes of the current study, which is the investigation of durability on jacket thickness, the approach detailed by Seible and Karbhari (1997) and Seible et al. (1997) will be used as an example. It is emphasized that the time dependent change in material properties (as listed in Table 4) could just as easily be used with other design approaches.

Since the design approach and equations are detailed in previously published work (Seible and Karbhari, 1997; Seible et al., 1997) they are not repeated herein. Rather only the pertinent final equations are provided to facilitate ease of reference. In each case the time dependent material properties $f_j(\tau)$, $E_j(\tau)$ and $\epsilon_j(\tau)$, for the strength, modulus and strain, respectively, will be used.

The jacket thickness for shear retrofit is determined as

$$t_j^v = \frac{\frac{V_o}{\phi_v} - (V_c + V_s + V_p)}{\frac{\pi}{2} \times 0.004 E_j(\tau) D} \quad \dots(4a)$$

for circular columns, and

$$t_j^v = \frac{\frac{V_o}{\phi_v} - (V_c + V_s + V_p)}{2 \times 0.004 E_j(\tau) D} \quad \dots(4b)$$

for rectangular columns, where V_o is the column shear demand based on full flexural over-strength in the potential plastic hinge regions, ϕ_v is the shear capacity reduction factor, assumed to be 0.85 in this study, V_c , V_s , and V_p are the shear capacity contributions related to concrete, horizontal steel reinforcement and axial load, respectively, as formulated in the three component shear model (Priestley et al., 1996), $E_j(\tau)$ is the time dependent value of the composite jacket modulus in the hoop direction (as described in Table 4), and D is the column dimension in the loading direction. The increase in shear strength in the section is achieved by constraining the opening of inclined cracks and with it the loss of aggregate interlock within these cracks through limiting the column dilation in the loading direction to less than 0.4% (Priestley et al., 1996).

In the case of flexural hinge confinement, for circular columns, the confinement effects are provided by the radial pressure forces generated by the jacket curvature and the tensile hoop strains in the jacket generated by the dilation of the plastic hinge. For rectangular columns with a side aspect ratio of depth/width < 1.5 and for columns with side dimensions of depth/width = 0.75/0.5 m, composite jackets with twice the theoretical thickness derived for an equivalent circular column of diameter D_c have performed well (Seible and Karbhari, 1997). Ductility of the flexural plastic hinge may also be increased through confinement of the region. The required jacket thickness for confinement of the flexural plastic hinge for circular columns is determined from

$$t_j^{c1} = 0.09 \frac{D(\epsilon_{cu} - 0.004) f_{cc}'}{\phi_f f_{ju}(\tau) \epsilon_{ju}(\tau)} \quad \dots(5)$$

where f_{cc}' is the confined concrete compression strength (while a number of empirical formulae have been proposed for this, a conservative value can be estimated as $1.5 f_c'$ (Priestley et al, 1996)), $f_{ju}(\tau)$ is the time de-

pendent strength capacity of the composite jacket in the hoop direction, $\epsilon_{ju}(\tau)$ is the time dependent strain of the composite jacket in the hoop direction (as described in Table 4), ϕ_f is the flexural capacity reduction factor (assumed to be 0.9), ϵ_{cu} is the ultimate concrete strain which depends on the confinement provided by the jacket and for purposes of design is determined by moment-curvature analysis as the product of ultimate section curvature and the corresponding neutral axis depth. These can both be determined from a sectional moment-curvature analysis and can be related to the ductility factor, μ_Δ , such that

$$\epsilon_{cu} = \mu_\Delta \Phi_y c_u \quad \dots(6)$$

The jacket thickness in the secondary confinement region, t_j^{c2} , is taken as half the value determined in the primary region through equation (5). It is noted that in the case of a rectangular jacket the thicknesses are approximated by doubling those determined for an equivalent circular column of diameter D_c . The relative slippage of concrete that adheres to the starter bars and the column reinforcement can be controlled with lap splice clamping using increased confinement to raise the shear-type friction. Experimental tests show an onset of debonding between 1,000 ___ and 2,000 ___ (Priestley et al., 1996). The dilation strain levels are often therefore conservatively limited to 1,000 ___, and the required jacket thickness is given by

$$t_j^s = 500 \frac{D(f_l - f_h)}{E_j(\tau)} \quad \dots(7)$$

where f_h is the horizontal stress level provided by the existing hoop reinforcement in a circular column at a strain of 0.1% given by

$$f_h = \frac{0.002 A_h E_h}{D_s} \quad \dots(8)$$

f_l is the lateral clamping pressure over the lap splice length, L_s and is determined as

$$f_l = \frac{A_s f_{sy}}{\left[\frac{p}{2n} + 2(d_b + c_c) \right] L_s} \quad \dots(9)$$

where p is the perimeter of the cross-section determined by the location of the lap-spliced steel reinforcement, n is the number of starter bars, d_b is the bar diameter, c_c is the concrete cover and L_s is the lap splice length provided in the steel reinforcement.

Since the intent of this investigation is to assess the effect of FRP material deterioration over time, rather than the equations used for design, in place of the conventionally used design form of a conservative estimate as $1.5 f_c'$ following Priestley et al. (1996), we use the empirical form proposed by Lam and Teng (2002) where

$$f'_{cc} = f'_c \left(1 + 2 \frac{f_l}{f'_c} \right) \quad \dots(10a)$$

wherein the lateral confinement provided by the composite jacket is estimated as

$$f_l = \frac{2f_{ju}(\tau)t}{d} \quad \dots(10b)$$

where t and d are the appropriately selected jacket thickness and diameter respectively.

Application to Jacket Design

For purposes of elucidation of the effect of environmental deterioration on assessment of jacket thickness, 4 different specimen configurations are used, some of which have been previously described in Seible and Karbhari (1997) and Seible et al. (1997), and were tested on 40% scale models as reported by Innamorato and Karbhari (2001). The specimen geometry and reinforcement details are provided in Table 6. For purposes of jacket design a displacement ductility level of at least 8 was required. For purposes of comparison results for jacket thickness are determined in each case using time dependent values for hoop strength, modulus and strain determined using the accelerated test determined equations reported in Table 4 and equations (10a) and (10b) to determine the value of the confined concrete strength, f'_{cc} in the time-dependent case to enable changes to be made in this value as well due to deterioration in hoop strength.

Case 1: Shear Retrofit of a Circular Column in Double Bending

The required jacket thickness inside and outside the plastic hinge region can be calculated from equations (4a) and (4b), respectively. Results for the three systems are shown in Figures 1(a)-(c). As can be seen from Figures 1(a)-(c) in all cases the effects of deterioration as related to the thickness required for shear retrofit are more pronounced in the first few years, with changes being relatively small after the initial period of time. However, the change in thickness required for flexural confinement is significantly greater, indicating the faster rate of deterioration in hoop strength and strain as compared to modulus. Based on the requirements of retrofit there are essentially 4 distinct zones along the height of the column: (1) L_{c1}^b and L_{c1}^t , the primary confinement regions for the plastic hinge, at the bottom and top of the column, respectively, extending a distance of 0.5D (or 304.8 mm in this case) each, (2) L_{c2}^b and L_{c2}^t , the secondary confinement regions for the plastic hinge, at the bottom and top of the column, respectively, extending a distance of 0.5D (or 304.8 mm in this case) each, (3) L_v^i , the shear strength region inside the plastic hinge region, both at the top and the bottom extending a distance of 1.5D (or 914.4 mm in this case), which essentially over-

laps and extends past the confinement region for the plastic hinge, and (4) L_v^o , the region of shear retrofit outside the plastic hinge region, spanning a distance of $H - 2L_v^i$ (or 609.2 mm in this case). Thus within the plastic hinge region the design thickness will be the larger of t_j^{c1} , t_j^{c2} and t_j^{vi} in the overlap region. As seen in Figure 1(a) in the case of Material A t_j^{c1} is always greater than t_j^{vi} , whereas t_j^{c2} is less than t_j^{vi} for a period of 9.3 years (at which point the required jacket thickness is 5.19 mm), after which the levels of material deterioration cause t_j^{c2} to be the operative thickness. In the case of Material B (Figure 1(b)) t_j^{c1} is less than t_j^{vi} for 11.8 years (at which point the required thickness is 6.93 mm) after which t_j^{c1} is the operative thickness. The thickness required in the secondary confinement region for the plastic hinge, t_j^{c2} , is always less than that required for shear retrofit, t_j^{vi} , and hence t_j^{vi} is used as the required thickness. In the case of Material C, the requirements for t_j^{vi} always dominate and hence this thickness is used over the entire plastic hinge region.

It is noted that the overall change in thickness as related to shear retrofit outside the plastic hinge region over even the extended period of 50 years is fairly small and the required increase is essentially less than the thickness of a single layer of additional material. Considering that the initial thickness of the jacket in the field is predicated by the number of layers of material used it is highly likely that the as-built thickness would more often than not be greater than that required even considering deterioration over the 50 year time period considered as an example in this investigation. As noted earlier, this however, does not hold true for jacket thickness required in regions of plastic hinge confinement. System C shows the best overall performance (i.e. the minimum change in thickness with time) whereas system A is the worst as related to the areas requiring shear retrofit, and system B is the worst in areas requiring flexural confinement. A comparison of values for thicknesses clearly shows the conservatism associated with the use of the ACI criteria even as compared to the 50-year predictions.

Case 2: Shear Retrofit of a Rectangular Column in Double Bending

Using a shear capacity reduction factor of $\phi_v = 0.85$, the required jacket thickness inside and outside the plastic hinge region can be calculated from equations (4a) and (4b), respectively, using the time-dependent equations for each of the three material systems, and are

shown in Figures 2(a)-(c) for the three material systems. To develop the full column capacity at the required displacement ductility of $\mu_\Delta = 8$, the required curvature ductility following equation (6) is 15, leading to an ultimate concrete strain, following equation (8) of 0.0095 mm/mm. The jacket thickness required to provide this level of ultimate concrete strain can be determined from equation (5) with the modification of multiplying the equation by 2 in consideration of the rectangular cross-section with the equivalent diameter dimension being determined through ovalization as 766 mm. Since $M/(VD) = L/D$ is less than 4 no anti-bar buckling thickness has to be added.

As seen in Figure 2(a) in the case of Material A, in the plastic hinge region t_j^{c1} and t_j^{c2} are always greater than t_j^{vi} . In the case of Material B (as seen in Figure 2(b)) t_j^{vi} has a larger requirement than t_j^{c1} only for a very short period of time of 0.1 year, at which point the required jacket thickness is 4.8 mm, whereas t_j^{c2} is less than t_j^{vi} for a period of 16.9 years (at which point the required jacket thickness is 5.09 mm). As in the case of the circular column, discussed previously in Case 1, the requirements for jacket thickness resulting from shear retrofit demands dominate even in the plastic hinge region for Material C.

Case 3: Flexural Retrofit of a Rectangular Cantilever Column

Using a shear capacity reduction factor of $\phi_v = 0.85$, the required jacket thickness inside and outside the plastic hinge region can be calculated from equations (4a) and (4b), respectively, using the time-dependent equations for each of the three material systems, and are shown in Figures 3(a)-(c) for the three material systems. To develop the full column capacity at the required displacement ductility of $\mu_\Delta = 8$, the required curvature ductility following equation (6) is 20.7, leading to an ultimate concrete strain, following equation (8) of 0.0202 mm/mm. The jacket thickness required to provide this level of ultimate concrete strain can be determined from equation (5), with the modification of multiplying the equation by 2 in consideration of the rectangular cross-section with the equivalent diameter dimension being determined through ovalization as 915 mm. In this case, both Materials A and B show the clear dominance of flexural confinement demands in the plastic hinge region (as seen in Figures 3(a) and 3(b)), with t_j^{c1} and t_j^{c2} always being greater than t_j^{vi} . However, in the case of Material C the jacket requirements in the secondary confinement region within the plastic hinge region, t_j^{c2} , is

less than that required for shear retrofit, t_j^{vi} , in that region for the short period of 0.3 years (at which point the required thickness is 4.97 mm).

From a practical perspective, the thickness required in the plastic hinge region for Materials A and B are significant and may in fact cause problems in ensuring adequate quality of performance in the field. In the case of Material A this concern is related to the excessive number of adhesive bonds required and the problems with ensuring compaction and uniform bond-line formation across that thickness, whereas in the case of Material B the concerns are associated with the larger number of inter-layer interfaces which have been shown in previous research (Abanilla et al, 2006) to result in faster deterioration due to environmental exposure. In this case, the significantly lower jacket requirements of Material C are a tremendous advantage from multiple perspectives.

Case 4: Lap-Splice Clamping of Circular Flexural Cantilever Column

Using a shear capacity reduction factor of $\phi_v = 0.85$, the required jacket thickness inside and outside the plastic hinge region can be calculated from equations (4a) and (4b), respectively, using the time-dependent equations for each of the three material systems, and are shown in Figures 4(a)-(c) for the three material systems. To develop the full column capacity at the required displacement ductility of $\mu_\Delta = 8$, the required curvature ductility following equation (6) is 22.6, leading to an ultimate concrete strain, following equation (8) of 0.0302 mm/mm. The jacket thickness required to provide this level of ultimate concrete strain can be determined from equation (5). Since L/D is greater than 4 in this case, the anti-bar buckling criteria needs to be checked, but can be shown to result in no additional jacket thickness.

In the case of lap-splice clamping retrofit of the circular flexural column, a further region of the jacket pertaining to lap-splice clamping, t_s , has to be considered. This region extends beyond the primary confinement region and into the secondary confinement region. Thus at the bottom of the column considered in this example, the designer has to consider jacket requirements in terms of four thicknesses, namely, t_s , t_j^{c1} , t_j^{c2} , and t_j^{vi} . As seen in Figure 4(a), for Material A, the requirement for jacket thickness pertaining to primary confinement in the plastic hinge dominates over the lap splice clamping requirement (i.e. $t_j^{c1} > t_s$) whereas the opposite is true in the secondary confinement region (i.e. $t_j^{c2} < t_s$). The thickness required for shear retrofit in the plastic hinge region is the least of the four, and can be seen to be significantly smaller at all levels than the other thickness requirements. It is noted that it is only 7.1% of the thickness required for primary confinement in the plastic

hinge region at the “unexposed” level and 4.1% at the 50-year level. As shown in Figure 4(b), in the case of Material B, $t_s > t_j^{c1}$ for a period of 40.1 years (at which point the jacket thickness is 22.42 mm in this region) and $t_s > t_j^{c2}$ over the entire 50-year period considered. In fact the thickness requirement for lap-splice clamping dominates over all others. This is also true in the case of Material C.

Summary And Conclusions

The durability of 3 FRP composite systems used for seismic retrofit of columns is investigated through tests conducted on ring-type specimens which have been shown to enable an assessment of both materials and structural level characteristics. Accelerated aging is enabled through the immersion of specimens in water at 4 different temperatures, three of which are used to determine predictions for long-term durability in terms of tensile strength, modulus and ultimate strain. To enable ease of use in design the predictions are developed as equations in the form

$$\frac{P(t)}{P_0} = A + B \ln(\tau) \quad \dots(11)$$

where $P(t)$ and P_0 are the characteristic at time t and 0, respectively, A and B are constants, with B representing the rate of degradation with time, τ , in days. Comparisons of predicted data at an immersion temperature of 23°C with field exposure results from Seattle-Tacoma are used to derive correlation factors between the laboratory and field. For the specific field exposure considered the two are fairly close. The time-dependent equations for materials response are then used in conjunction with equations for determination of FRP jacket thickness for seismic retrofit, and it is shown that the use of the time-dependent approach provides a better estimate of thickness in the different regions of the columns and even enables an assessment of periods in which one set of demands may override others. This approach thus allows designers to appropriately detail jackets based on estimated service-life requirements, and also provide ease of comparison between material systems. Results are elucidated through 4 different retrofit scenarios, and the efficacy of each of the three material systems is demonstrated and compared. Comparison of thicknesses resulting from the use of the time-dependent approach with the thicknesses resulting from the use of the ACI-440 (2002) recommendations for durability suggest that the ACI approach is overly conservative in this case, which could result in the development of inefficient and cost-prohibitive designs.

References

Abanilla, M.A., Karbhari, V.M. and Li, Y (2006, in press), “Interlaminar and Intralaminar Durability
COMPOSITES 2006

- Characterization of Wet Layup Carbon/Epoxy Used in External Strengthening, Composites B.
American Concrete Institute, (2002), “Guide for the Design and Construction of Externally Bonded FRP Systems for Strengthening Concrete Structures,” ACI Committee 440, Report 440.2R-02, American Concrete Institute, Farmington Hills, MI.
California Department of Transportation (1996), Caltrans Memorandum to Designers, 20-4, Attachment B: Composite Column Casing, and Standard Specification. I.48_AENC.DOC.
Chin, J.W., Hughes, W.L. and Signor, A. (2001), “Elevated Temperature Aging of Glass Fiber Reinforced Vinyl Ester and Isophthalic Polyester Composites in Water, Salt Water and Concrete Pore Water Solutions,” Proceedings of the 16th ASCE Conference, American Society of Composites, Dayton, OH.
Innamorato, D. and Karbhari, V.M. (2002), “FRP Composite Wrap Durability Evaluation: Volume 2 – Structural Test Results Summary,” University of California San Diego, Structural Systems Research Project, Report no. TR-2001/11.
Karbhari, V.M., Zhang, J., Wu, L. and Reynaud, D. (2003), “Materials and Durability Characterization of Composite Wrap Systems Using NOL Ring Tests,” in *Composite Materials: Testing and Design Fourteenth Volume, ASTM STP 1436*, C. E. Bakis, Ed., American Society for Testing and Materials, West Conshohocken, PA, 2003, pp. 151-165.
Karbhari, V.M. (2004), “E-Glass/Vinylester Composites in Aqueous Environments: Effects on Short-Beam Shear Strength,” *ASCE Journal of Composites for Construction*, 8[2], pp. 148-156.
Lam, L. and Teng, J.G. (2002), Strength Models for FRP-Confined Concrete, *ASCE Journal of Structural Engineering*, 128[5], pp. 612-623.
Litherland, K.L., Oakley, D.R. and Proctor, B.A. (1981), “The Use of Accelerated Ageing Procedures to Predict the Long-Term Strength of GRC Composites,” *Cement and Concrete Research*, 11, pp. 455-466.
Mirmiran, A., Shahawy, M., Nanni, A. and Karbhari, V.M. (2004), “Bonded Repair and Retrofit of Concrete Structures Using FRP Composites: Recommended Construction Specifications and Process Control Manual,” NCHRP-514, Transportation Research Board, National Academy Press.
Pantelides, C.P., Gergely, J. and Reaveley, L.D. (1999), “Retrofit of RC Bridge Pier With CFRP Composites,” *ASCE Journal of Structural Engineering*, 125[10], pp. 1094-1099.
Pantelides, C.P. and Gergely, J. (2002), “Carbon-Fiber-Reinforced Polymer Seismic Retrofit of RC Bridge Bent: Design and In Situ Validation,” *ASCE Journal of Composites for Construction*, 6[1], pp. 52-60.
Pantelides, C.P., Alameddine, F., Sardo, T. and Imbsen, R. (2004), “Seismic Retrofit of State Street Bridge on Interstate 80” *ASCE Journal of Bridge Engineering*, 9[4], pp. 333-342.

Priestley, M.J.N. and Seible, F. (1995), "Design of Seismic Retrofit Measures for Concrete and Masonry Structures," *Construction and Building Materials*, 9[9], pp. 365-377.

Priestley, M.J.N., Seible, F. and Calvi, M. (1996), *Seismic Design and Retrofit of Bridges*, John Wiley & Sons Inc., New York.

Proctor, B.A., Oakley, D.R. and Litherland, K.L. (1982), "Developments in the Assessment and Performance of GRC Over 10 Years," *Composites*, 13[2], 73.

Reynaud, D., Karbhari, V.M. and Seible, F. (1999), "The HITEC Evaluation Program for Composite Column Wrap Systems for Seismic Retrofit," *International Composites Exposition '99*, Cincinnati, OH, pp. 4A/1-6.

Saenz, N., Walsh, E.J., Pantelides, C.P. and Adams, D.O. (2005a), "Long Term Durability of FRP Composites for Infrastructure Rehabilitation," *Proceedings of the SAMPE Conference*, Long Beach, Ca, 12 pp.

Saenz, N., Pantelides, C.P. and Reveley, L.D. (2005b), "Long Term Durability of Strengthened Concrete With Externally Applied FRP Composites," *Proceedings of the SAMPE Conference*, Long Beach, Ca, 12 pp.

Saïidi, M.S., Martinovic, F., McElhaney, B., Sanders, D. and Gordaninejad, F. (2004), "Assessment of Steel and Fiber Reinforced Plastic Jackets for Seismic Retrofit of Reinforced Concrete Columns With Structural Flares," *ASCE Journal of Structural Engineering*, 130[4], pp. 609-617.

Seible, F. and Karbhari, V.M. (1997) "Seismic Retrofit of Bridge Columns Using Advanced Composite Materials," *The National Seminar on Advanced Composite Material Bridges*, May 5-7, Washington, D.C., 1-29 pp.

Seible, F., Priestley, M.J.N., Hegemier, G.A. and Innamorato, D. (1997), "Seismic Retrofit of RC Columns With Continuous Carbon Fiber Jackets," *ASCE Journal of Composites for Construction*, 1[2], pp. 40-52.

Teng, J.G., Chen, J.F., Smith, S.T. and Lam, L. (2002), *FRP Strengthened RC Structures*, Wiley, 2002.

TR-55 (2000), "Design Guidance for Strengthening Concrete Structures Using Fibre Composite Materials," *The Concrete Society*, UK.

Xiao, Y. and Ma, R. (1997), "Seismic Retrofit of RC Circular Columns Using Prefabricated Composite Jacketing," *ASCE Journal of Structural Engineering*, 123[10], pp. 1357-1364.

Zhang, J.S., Karbhari, V.M., Isley, F. And Neuner, J. (2003a), "Fiber-Sizing-Based Enhancement of Materials Durability for Seismic Retrofit," *ASCE Journal of Composites for Construction*, 7[3], pp. 194-199.

Zhang, J.S., Karbhari, V.M., Wu, L. and Reynaud, D. (2003b) "Field Exposure Based Durability Assessment of FRP Column Wrap Systems," *Composites B*, Vol. 34[1], pp. 41-50.

Table 1: % Retention of System A Properties

Exposure: Immersion in Deionized Water		Hoop Strength	Hoop Modulus	Strain
Unexposed Baseline		386.00 MPa	40.70 GPa	9250 _ strain
15 °C	6 months	94%	99%	96%
	12 months	93%	98%	97%
	18 months	90%	98%	94%
	24 months	85%	97%	91%
23 °C	6 months	89%	96%	100.2%
	12 months	89%	91%	106.6%
	18 months	89%	93%	99.7%
	24 months	77%	90%	87%
40 °C	6 months	79%	93%	88%
	12 months	45%	75%	66%
	18 months	32%	66%	51%
	24 months	0%	0%	0%
60 °C	6 months	79%	90%	99.5%
	12 months	32%	30%	82%
	18 months	0%	0%	0%
	24 months	0%	0%	0%

Table 2: % Retention of System B Properties

Exposure: Immersion in Deionized Water		Hoop Strength	Hoop Modulus	Strain
Unexposed Baseline		468.90 MPa	28.80 GPa	17992 _ strain
15 °C	6 months	91%	100%	96%
	12 months	80%	95%	85%
	18 months	66%	92%	75%
	24 months	64%	91%	72%
23 °C	6 months	89%	104%	96%
	12 months	76%	94%	72%
	18 months	65%	89%	68%
	24 months	61%	91%	67%
40 °C	6 months	70%	103%	68%
	12 months	66%	92%	64%
	18 months	54%	95%	56%
	24 months	46%	90%	53%
60 °C	6 months	50%	104%	43.5%
	12 months	50%	104%	43.5%
	18 months	46%	94%	42.9%
	24 months	40%	90%	41%

Table 3: % Retention of System C Properties

Exposure: Immersion in Deionized Water		Hoop Strength	Hoop Modulus	Strain
Unexposed Baseline		606.80 MPa	26.30 GPa	22343 μ -strain
15 °C	98%	100%	99.0%	96%
	95%	99%	98.0%	85%
	90%	97%	95.0%	75%
	88%	96%	92.0%	72%
23 °C	85%	92%	88.3%	96%
	83%	92%	90.7%	72%
	81%	93%	86.4%	68%
	78%	91%	86.1%	67%
40 °C	66%	94%	70.2%	68%
	65%	93%	62.1%	64%
	60%	90%	56.3%	56%
	46%	88%	55.0%	53%
60 °C	38%	92%	37.9%	43.5%
	37%	94%	38.1%	43.5%
	37%	98%	35.5%	42.9%
	33%	90%	31.1%	41%

Table 4 Predictive Equations (expressed as $P(t) / P_0 = A + B \ln(\tau)$ where P(t) is the property at any time $t > 0$, P_0 is the unexposed value at $t = 0$, A and B are constants, with B representing the rate of degradation with time, and τ is the time in days)

Characteristic	System	Predictive Equation
Strength, $f_j(\tau)$	A	$=1.0339-0.0403 \ln(\tau)$
	B	$=1.0029-0.0525 \ln(\tau)$
	C	$=1.0363-0.0375 \ln(\tau)$
Modulus, $E_j(\tau)$	A	$=1.0014-0.0163 \ln(\tau)$
	B	$=1.0012-0.0097 \ln(\tau)$
	C	$=1.0110-0.0089 \ln(\tau)$
Strain, $\epsilon_j(\tau)$	A	$=1.0031-0.0250 \ln(\tau)$
	B	$=1.0022-0.0439 \ln(\tau)$
	C	$=1.0294-0.0318 \ln(\tau)$

Table 5: Values for Material Parameters

	System	f_{ju} (MPa)	E_{ju} (GPa)	ϵ_{ju} (μ Strain)
“Un-exposed”	A	386	40.7	9250
	B	468.9	28.8	17992
	C	606.8	26.3	22343
ACI-440 at $C_E = 0.65$	A	224.01	24.45	4947.8
	B	251.00	16.83	8461.7
	C	380.98	16.16	13220.4
Time in years to reach the ACI 440 Values	A	14.8	> 100	> 100
	B	20.5	> 100	> 100
	C	> 100	> 100	> 100

Table 6: Summary of Material, Configuration Details and Specifications for Columns

Characteristic	Shear in Double Bending	Shear in Double Bending	Flexure	Lap Splice in Flexure
Column Section				
c/s	Circular	Rect.	Rect.	Circular
H (mm)	2438	2438	3658	3658
L (mm)	1219	1219	3658	3658
D (mm)	609.6	609.6	730	609.6
B (mm)	609.6	406	489	609.6
cc (mm)	20.32	19	19	19
f'_c (MPa)	34.45	34.45	34.45	34.45
P (kN)	591.85	507	1780	1780
M_{vi} (kN.m)	647	619	2165	815
Φ_y (1/mm)	5.984×10^{-6}	5.472×10^{-6}	4.685×10^{-6}	6.339×10^{-6}
c_u (mm)	152.4	116	208	211
Longitudinal Reinforcement (Grade 40)				
d_b (mm)	19 (#6)	19 (#6)	25 (#8) 22 (#7)	19 (#6)
n	26	22	14 28	26
A_s (mm ²)	284	284	510	284
f_{sv} (MPa)	303.16	303.16	303.16	303.16
Transverse Reinforcement (Grade 40)				
d_b (mm)	6 (#2)	6 (#2)	6 (#2)	6 (#2)
A_h (mm ²)	32	32	32	32
s (mm)	127	127	127	127

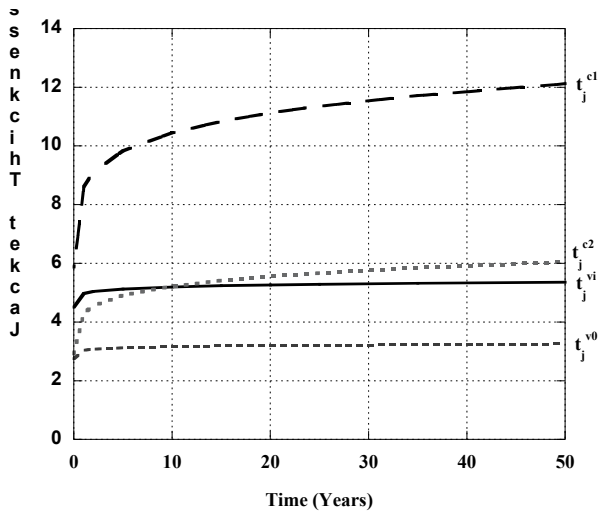


Figure 1(a): Material A based jacket thicknesses for circular column to be retrofit for shear in double bending

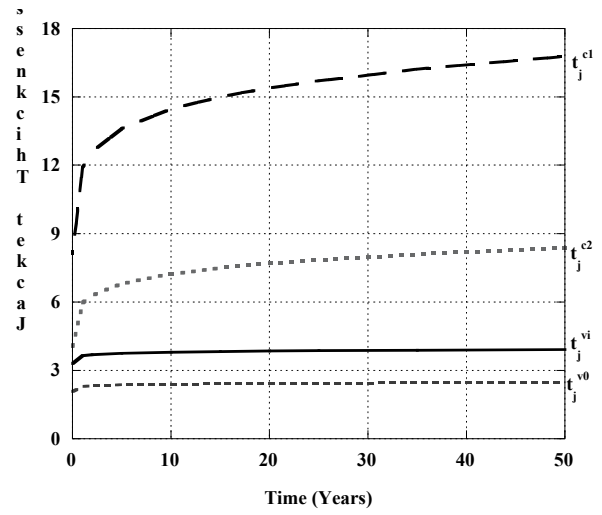


Figure 2(a): Material A based jacket thicknesses for rectangular column to be retrofit for shear in double bending

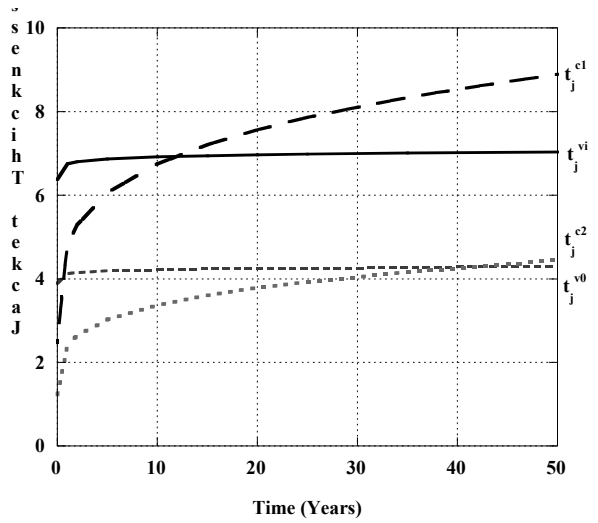


Figure 1(b): Material B based jacket thicknesses for circular column to be retrofit for shear in double bending

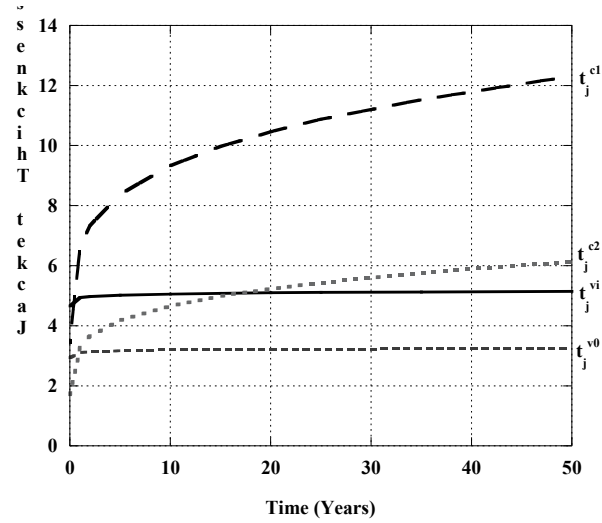


Figure 2(b): Material B based jacket thicknesses for rectangular column to be retrofit for shear in double bending

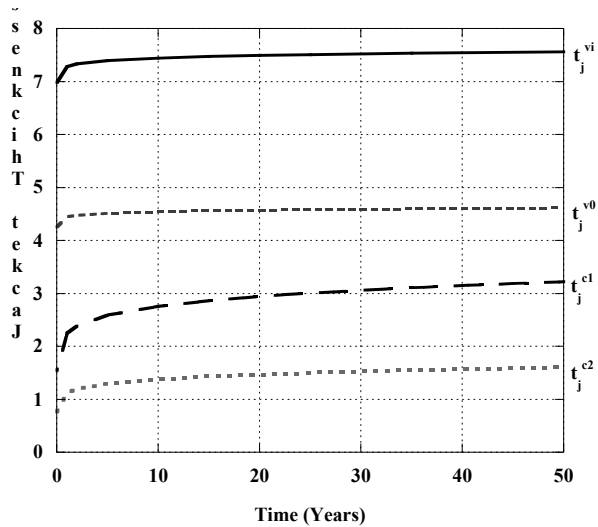


Figure 1(c): Material C based jacket thicknesses for circular column to be retrofit for shear in double bending

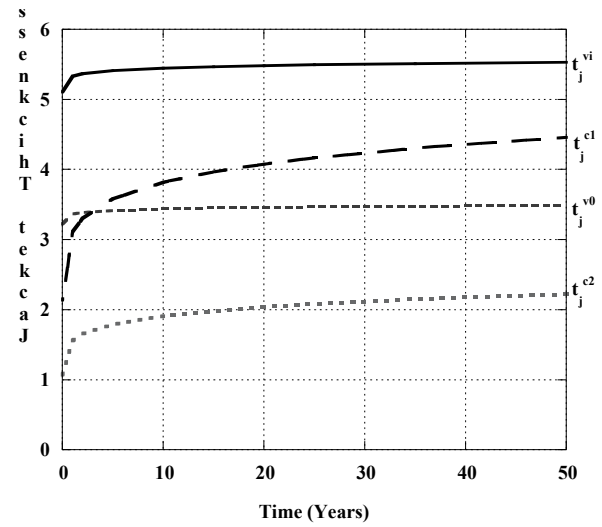


Figure 2(c): Material C based jacket thicknesses for rectangular column to be retrofit for shear in double bending

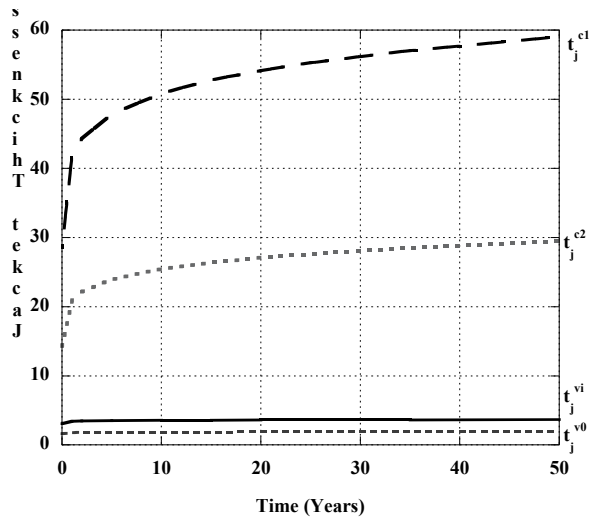


Figure 3(a): Material A based jacket thicknesses for rectangular column to be retrofit for flexure

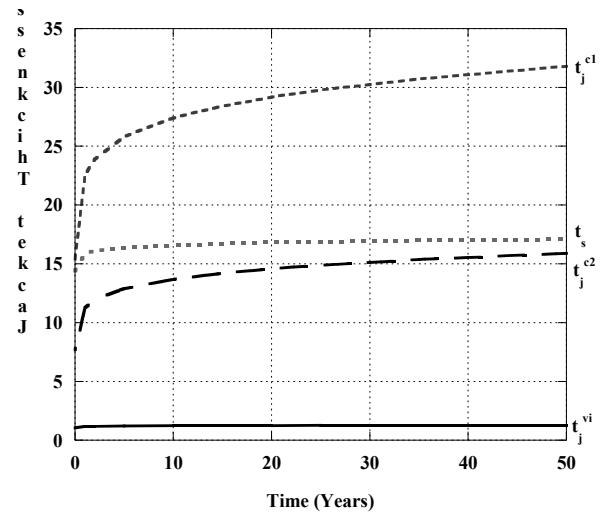


Figure 4(a): Material A based jacket thicknesses for circular column to be retrofit for lap-splice in flexure

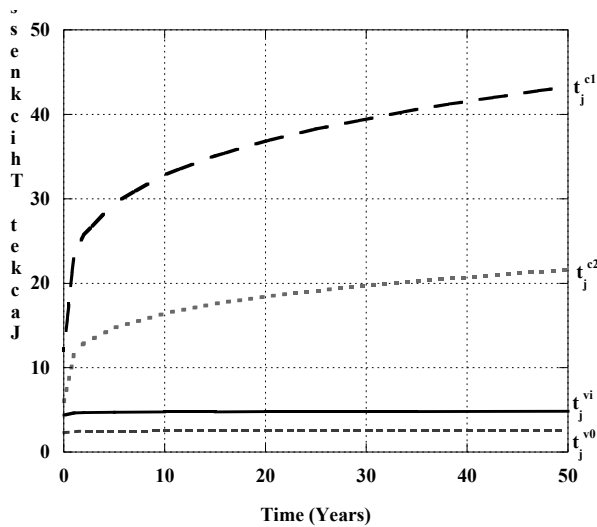


Figure 3(b): Material B based jacket thicknesses for rectangular column to be retrofit for flexure

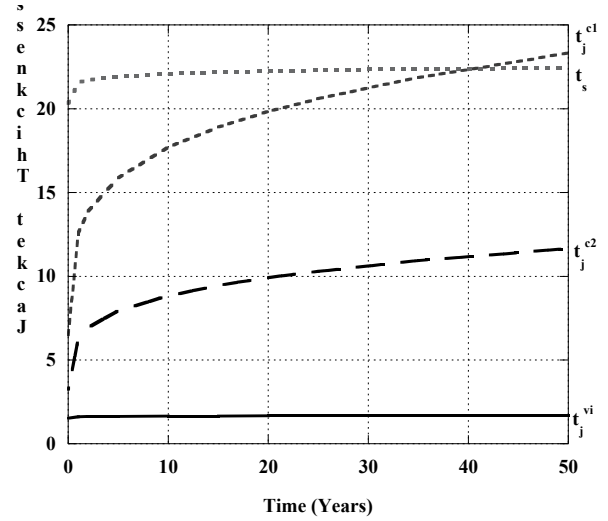


Figure 4(b): Material B based jacket thicknesses for circular column to be retrofit for lap-splice in flexure

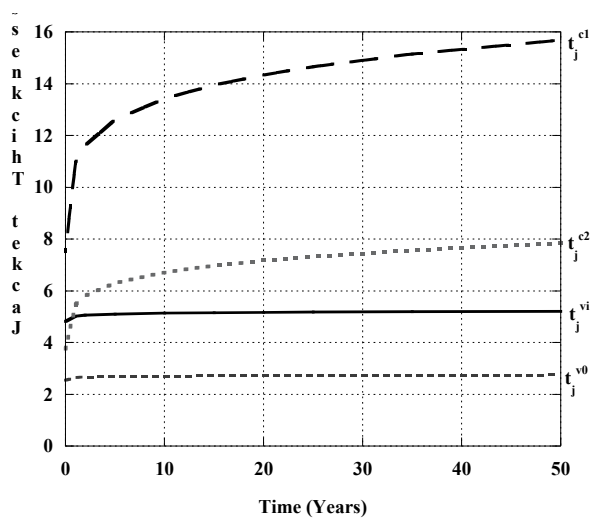


Figure 3(c): Material C based jacket thicknesses for rectangular column to be retrofit for flexure

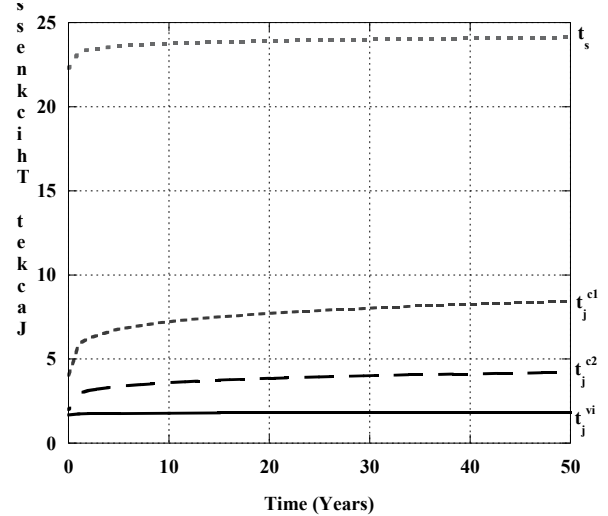


Figure 4(c): Material C based jacket thicknesses for circular column to be retrofit for lap-splice in flexure